



# One dimensional photonic crystal structure comprising a hyperbolic metamaterial for optical filtering purpose

Z. A. Alrowaili<sup>1</sup> · Mai Medhat<sup>2</sup> · T. A. Taha<sup>1</sup> · Ahmed Mehaney<sup>2</sup> · Lama Sh. Aljoufi<sup>3</sup> · Hussein A. Elsayed<sup>2</sup>

Received: 9 May 2022 / Accepted: 11 October 2022 / Published online: 22 November 2022  
© The Author(s), under exclusive licence to Springer Science+Business Media, LLC, part of Springer Nature 2022

## Abstract

In this research, we have theoretically introduced a model structure of one-dimensional photonic crystals to act as a multichannel optical filter. The suggested design is composed of a periodic alteration of hyperbolic metamaterial (HMM) and SiO<sub>2</sub> layers. The HMM is composed of a combination of Si and Ag layers. Meanwhile, our design is configured as [(Si/Ag)<sup>N</sup>SiO<sub>2</sub>]<sup>S</sup>. The theoretical treatment is substantially demonstrated in the vicinity of the characteristic matrix method, effective medium theory, and the Drude model. The numerical findings have demonstrated the effects of the periodicity numbers (N and S), the thicknesses of the Ag and Si layers, and the refractive index of SiO<sub>2</sub> on the structure filtering properties. In this regard, the numerical findings clarify that the periodicity number of the HMM is a crucial parameter in introducing a specified number of filter channels. Our designed structure may help in the enhancement of photonic and optical applications such as a multichannel filter, particularly via a wide range of visible light regions.

**Keywords** Photonic crystals · Photonic band gaps · Hyperbolic metamaterial · Characteristic matrix method · Multichannel optical filter

## 1 Introduction

Since Eli-Yablonovitch and John established the principles of the interaction between electromagnetic waves and some artificial periodic structures (Yablonovitch 1987; John 1987; Elsayed and Mehaney 2021; Devashish et al. 2019), photonic crystals (PCs) have received a lot of attention. These structures are heterogeneous and nanostructures with a periodic arrangement of their refractive indices to control the propagation of light (Joannopoulos et al. 2008). Their studies led to the formation of some regions or bands of frequency ranges in which the propagation of some electromagnetic frequencies is

---

✉ Z. A. Alrowaili  
zalrowaili@ju.edu.sa

<sup>1</sup> Physics Department, College of Science, Jouf University, P.O. Box: 2014, Sakaka, Saudi Arabia

<sup>2</sup> Physics Department, Faculty of Science, Beni-Suef University, Beni-Suef 62512, Egypt

<sup>3</sup> Department of Mathematics, College of Science, Jouf University, P.O. Box: 2014, Sakaka, Saudi Arabia

not allowed (Devashish et al. 2019; Joannopoulos et al. 2008). Meanwhile, these bands are labeled as photonic band gaps (PBGs) (Noda Baba 2003). Thus, the dominant cause around the appearance of these PBGs is the periodicity of the refractive indices in one, two, or three dimensions that lead to Bragg scattering at the interfaces of these periodic arrays (Sánchez and Halevi 2003; Elsayed and Mehanev 2019; Elsayed 2018a). In addition, the ability to localize some distinct wavelengths inside the created PBGs could be also of significant interest. Therefore, PCs could be promising in many scientific communities. In this context, PCs can be fabricated with a lattice constant compared to the incident wavelengths in one, two and three-dimension lattices (Yablonovitch 1987; John 1987; Elsayed and Mehanev 2021, 2019; Devashish et al. 2019; Joannopoulos et al. 2008; Noda Baba 2003; Sánchez and Halevi 2003; Elsayed 2018a). However, the designed PCs with a one-dimensional (1D) configuration may be the simplest in terms of manufacturing designs and theoretical approaches, specifically, there is a variety in the utilized materials to design or manufacture the 1D PC structures such as metals (Gaspar-Armenta and Villa 2003; Wu et al. 2010a), superconductors (), semiconductors (Noda et al. 2002; Istrate and Sargent 2006), liquid crystals (Trabelsi et al. 2020; Haakestad et al. 2005) and metamaterial (). Notably, the constituent materials of PCs could clearly tune the position and width of PBGs. Furthermore, several researchers have improved the properties of PBGs dependent upon many factors and influences like temperature, pressure (Elsayed et al. 2014; Porras-Montenegro and Duque 2010) and electric or magnetic fields (Wu et al. 2010b; Zheng et al. 2007; Aly et al. 2015; Xu et al. 2003; Aly and ElSayed 2016). Thus, the promising properties of PCs have contributed to many applications and devices such as optical filters, modulators (Notomi et al. 2005; Hadfield 2009), optical reflectors (Elsayed and Aly 2017), and switches (Takeda and Yoshino 2004).

Nowadays, there is an increasing interest in using some newly designed materials through PC structures named Metamaterials (MMs) (Huo et al. 2019; Ramanujam et al. 2019; Campione et al. 2020; Janaszek et al. 2018; Podolskiy et al. 2007; Correias-Serrano et al. 2015; Shalin et al. 2015). In particular, MMs have precise shape, geometry, specific orientation properties and negative refractive index (Huo et al. 2019). The existence of this new type of material was firstly demonstrated by Veslago (1968). Veslago deduced that these materials could provide new peculiar optical characteristics due to their negative refractive indices. Meanwhile, Smith et al. discussed experimentally the optical properties of such materials at microwave frequencies (Aghajamali and Barati 2013; Smith et al. 2000). In fact, the inclusion of MMs in PCs could be a crucial factor in tuning the PBG because the average index of refraction for the considered structure could be close to zero (Li et al. 2003). In addition, MMs provide the possibility for the enhancement of the incident electromagnetic waves besides the trapping of the electromagnetic field at some resonance frequencies (Cui et al. 2020). These features devoted attention to the utilization of MMs in some sensing applications like label-free DNA sensing (Haring Bolivar et al. 2004), thermal induced denaturation temperature of insulin (Li et al. 2020), and chemical sensing as well (Drexler et al. 2014).

Recently, a new class of these materials called hyperbolic metamaterials (HMMs) has been widely considered due to their indefinite dispersion (Ramanujam et al. 2019). Notably, it could be designed in the form of dielectric-metal multilayers (Ramanujam et al. 2019). In addition, HMMs can be used in a variety of applications such as uniaxial media with anisotropic permittivity tensors that have opposite signs to the axial and tangential components (Huo et al. 2019). It is very important to note that the HMM structure has a naturally dissipative loss lower than the pure bulk metallic structure (Huo et al. 2019). In fact, the response of HMMs structure to electromagnetic waves could be demonstrated

based on the effective medium theory (EMT) which traps only the temporal dispersion and depends on the frequency effective electric permittivity tensor (Ramanujam et al. 2019; Campione et al. 2020; Janaszek et al. 2018). Moreover, HMMs are used in many applications to achieve the growth of angle insensitive PBGs (Podolskiy et al. 2007). In most PC structures that have HMMs, we looked at the PC and how the PBG looks in permeability, permittivity, and negative refractive index (Correas-Serrano et al. 2015; Shalin et al. 2015). Therefore, HMMs are pioneering in the design and fabrication of many different applications such as hyperlenses and high-sensitivity sensors as well (Guo et al. 2020). In particular, the high  $k$  modes in HMMs can overcome the diffraction limit unlike the conventional lens besides being effective materials towards the small changes in the refractive index of the sensing medium (Guo et al. 2020).

Furthermore, PCs comprising HMMs were promising in the demonstration of angle insensitive or independent PBGs on both theoretical and experimental levels (Wu et al. 2018, 2022). Such gaps could be of potential interest in many applications like omnidirectional reflectors, phase shift controllers and solar cells applications. Moreover, the dispersionless cavity modes represent another motivation for HMMs through PC designs (Xue et al. 2016). In this regard, Xue et al. investigated that the spectral features of a cavity mode inside the dispersionless gap are almost invariant with incident angles (Xue et al. 2016). In addition, Hu et al. have considered the inclusion of magneto optical HMMs through PCs to investigate a nonreciprocal omnidirectional cavity mode (Hu et al. 2022). Recently, the formation of tri and tetra hyperbolic phases in anisotropic MMs without magnetoelectric coupling received a considerable attention (Durach 2020; Tuz and Fesenko 2020; Fesenko and Tuz 2019; Durach et al. 2020). Such improvements could be of a significant interest in many physical and technological aspects.

Based on all of these breakthroughs of HMMs, we have considered here the possibility of using this type of materials to design an optical multichannel filter in the visible light. Our idea is essentially based on the design of one-dimensional photonic crystals (1DPCs) comprising HMMs and dielectric material. In particular, the numerical findings can provide a wide control of the number of channels based on the number of periods for HMMs. To the best of our knowledge, such result could be of potential interest compared to the traditional designs of PCs. Notably, the design of a multichannel optical filter based on dielectric PCs could not provide full control over the number of channels. In addition, the ability to control the number of channels for the produced optical filter could need some special materials as investigated by Elsayed (2018b). Elsayed has introduced a multichannel optical filter for visible light applications using the 1D PCs that contain an n-doped InSb semiconductor material of a higher doping level. In this context, the doping impurity concentration was crucial in controlling the number of channels (Elsayed 2018b). As the doping impurity concentration increases, the permittivity of the n-doped semiconductors begins to receive large negative values. Such a response could produce a high contrast between the constituent materials of PCs (Elsayed 2018b). Thus, we believe that the inclusion of HMM in our design could play the same role without the needing for some special requirements. In particular, HMMs provide some peculiar optical characteristics compared to other dispersive media. Here, our design is configured as,  $[(Si/Ag)^N SiO_2]^S$ . In this regard, the number of periods  $N$  for the HMM plays the main role in increasing the number of channels for the investigated optical filter. The theoretical analysis of this work is mainly based on the characteristic matrix method and the well-known Drude model. Meanwhile, the numerical results indicate the existence of a multichannel optical filter in the visible light range. On one hand, we discuss the effects of many parameters such as the thickness of dielectric and metal layers on the filtering features of the PC structure. On the other hand, we pay more

attention to the effects of the periodicity number of the HMM on the produced number of the filter channels.

## 2 Theoretical analysis

Now, we briefly introduce the theoretical framework based on the characteristic matrix method to describe the influence of the electromagnetic waves through the designed 1DPCs. As shown in Fig. 1, the considered structure is composed of two alternating materials HMM (D layers) and dielectric (C layers) that are repeated for  $S$  periods in the whole structure. Meanwhile, HMM layers are designed from a multi-combination of two layers, A and B, with a repetition number  $N$ . Here, layers A and B are listed for dielectric and metallic media with thicknesses  $d_A, d_B$  and refractive indices  $n_A, n_B$ , respectively. Therefore, the whole structure can be mimicked as  $[(A/B)^N C]^S$ , and then it will be immersed between air and substrate. Meanwhile, layers A, B and C are considered Si, Ag and SiO<sub>2</sub>, respectively. These materials are widely used in the design of PCs due to many advantages. Ag is characterized by the low light absorption in the operating wavelengths of this study (visible light and near-ultraviolet regions). Also, SiO<sub>2</sub> has large stability in its refractive index value in this wavelength region. Besides, Si and SiO<sub>2</sub> are selected due to their unique optical and chemical properties, and abundance of fabrication techniques. Moreover, these materials are used extensively in previous theoretical and experimental PC applications. Thus, the suggested structure could be described as the following configuration,  $[(Si/Ag)^N SiO_2]^S$ . Then, the substrate is chosen as a glass of refractive index  $n_s = 1.52$ .

In this context, the transfer or characteristic matrix method is admitted for investigating the transmission spectra of the 1DPC containing the HMM (Elsayed 2018b; Elsayed and Mehaney 2020; Born and Wolf 1999). Through our analysis, we considered that the propagation of the electromagnetic waves is parallel to the  $x$ -direction. Thus, the electric and magnetic fields of electromagnetic waves will vibrate in the  $(y-z)$  plane. Therefore, the response of both the electric and magnetic field components through a single layer  $j$  of the proposed design is written as (Elsayed and Mehaney 2020; Born and Wolf 1999):

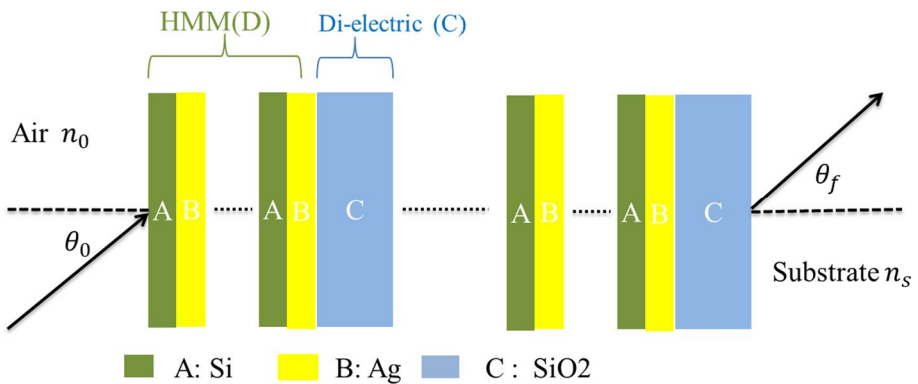


**Fig. 1** The schematic diagram of the 1D-PC containing HMM (A and B) layers and dielectric material (C) layer. Here, each layer has a certain thickness and characteristic refractive index. The refractive index of air and substrate is labeled as  $n_0, n_s$ , respectively

$$\begin{aligned}
 E_j &= A_j \exp(-ik_j x) + B_j \exp(ik_j x) = E_{y^+} + E_{y^-} \\
 H_j &= \frac{\partial E_j}{i\omega \partial x} = \frac{k_j}{\omega} [-A_j \exp(-ik_j x) - B_j \exp(ik_j x)] \\
 &= \frac{k_j}{\omega} (E_{y^+} - E_{y^-}) = Q_j (E_{y^+} - E_{y^-})
 \end{aligned}
 \tag{1}$$

such that,  $A_j$  and  $B_j$  are the field amplitudes in layer  $j$ ,  $k_j$  is the wave vector in layer  $j$ , and it is written as  $k_j = k_0 n_j \cos \theta_j = (2\pi/\lambda) n_j \cos \theta_j$ ,  $\lambda$  is the wavelength of incident waves,  $n_j$  and  $\theta_j$  describe the refractive index and angle of incidence through this layer, respectively. For simplicity, Eq. (1) could be written in the following form:

$$\begin{pmatrix} E_j \\ H_j \end{pmatrix} = \begin{pmatrix} 1 & 1 \\ Q_j & -Q_j \end{pmatrix} \begin{pmatrix} E_{y^+} \\ E_{y^-} \end{pmatrix}
 \tag{2}$$

Then, we can obtain:

$$\begin{pmatrix} E_{y^+} \\ E_{y^-} \end{pmatrix} = \frac{1}{2} \begin{pmatrix} 1 & Q^{-1} \\ 1 & -Q^{-1} \end{pmatrix} \begin{pmatrix} E_j \\ H_j \end{pmatrix}
 \tag{3}$$

For a distinct layer  $j$  of thickness  $d_j = x_1 - x_0$ , the response of the incident electromagnetic wave through their boundaries can be summarized as:

$$\begin{pmatrix} E_{y^{0+}} \\ H_{y^{0-}} \end{pmatrix} = \begin{pmatrix} \exp[ik_j d_j] & 0 \\ 0 & \exp[ik_j d_j] \end{pmatrix} \begin{pmatrix} E_{y^{1+}} \\ E_{y^{1-}} \end{pmatrix}
 \tag{4}$$

From Eqs. (2), (3) and (4), we have: -

$$\begin{aligned}
 \begin{pmatrix} E_0 \\ H_0 \end{pmatrix} &= \begin{pmatrix} 1 & 1 \\ Q_j & -Q_j \end{pmatrix} \begin{pmatrix} E_{y^{0+}} \\ H_{y^{0-}} \end{pmatrix} \\
 &= \begin{pmatrix} 1 & 1 \\ Q_j & -Q_j \end{pmatrix} \begin{pmatrix} \exp[ik_j d_j] & 0 \\ 0 & \exp[ik_j d_j] \end{pmatrix} \begin{pmatrix} E_{y^{1+}} \\ E_{y^{1-}} \end{pmatrix} \\
 &= \begin{pmatrix} \cos(k_j d_j) & (-i/Q_j) \sin(k_j d_j) \\ -iQ_j \sin(k_j d_j) & \cos(k_j d_j) \end{pmatrix} \begin{pmatrix} E_1 \\ H_1 \end{pmatrix} = w_j \begin{pmatrix} E_1 \\ H_1 \end{pmatrix}
 \end{aligned}
 \tag{5}$$

Therefore, the response of the incident waves through the whole periodic structure could be expressed in the vicinity of Eq. (5) as in the following matrix: -

$$W = \begin{pmatrix} W_{11} & W_{12} \\ W_{21} & W_{22} \end{pmatrix} = \prod_{j=1}^k w_j = (W_D W_C)^S = \left( (W_A W_B)^N W_C \right)^S
 \tag{6}$$

where  $W_A$ ,  $W_B$  and  $W_C$  are the characteristic matrices of (A, B and C) layers, respectively. While  $W_D$  represents the matrix of the HMM which included two matrices of dielectric and metal materials. Meanwhile, the matrix elements of Eq. (6) represent the mainstay in describing the transmittance coefficient of the constructed structure as represented in the following form: -

$$t = \frac{2p_0}{(W_{11} + W_{12} p_s) p_0 + (W_{21} + W_{22} p_s)}
 \tag{7}$$

Finally, the structure transmittance could be expressed based on the transmittance coefficient and the optical properties of the starting medium (air) and substrate as:

$$T = \frac{P_s}{P_0} |t^2| \tag{8}$$

Then, we investigated the refractive index of the HMM layer due to its construction as a combination of metallic and dielectric media. As mentioned above, for the metallic layer, we have considered Ag as it has the lowest light absorption compared with other metals in visible light and near-ultraviolet regions (Johnson and Christy 1972). According to Drude model, we can define the relative permittivity of Ag as the following equation:

$$\epsilon_B = \epsilon_{inf} - \frac{(\omega_p)^2}{\omega^2 + i\omega\gamma} \tag{9}$$

here  $\epsilon_{inf}$ ,  $\gamma$  and  $\omega_p$  are configured as the high-frequency relative permittivity, damping frequency and plasma frequency, respectively. In this context, the values of these parameters are obtained based on some experimental measurements such that,  $\epsilon_{inf} = 5.0$ ,  $\hbar\gamma = 0.0212eV$  and  $\hbar\omega_p = 9.2159eV$  (Johnson and Christy 1972; Zhao et al. 2014). According to the effective medium theory, the parallel and transverse components of the HMM permittivity could be expressed as (Poddubny et al. 2013): -

$$\epsilon_p = F\epsilon_A + (1 - F)\epsilon_B \tag{10}$$

$$\frac{1}{\epsilon_v} = \frac{F}{\epsilon_A} + \frac{1 - F}{\epsilon_B} \tag{11}$$

$$F = d_A / (d_A + d_B) \tag{12}$$

where  $F$  defines the filling factor of layer A relative to the HMM layer. Finally, the refractive indices of layers A (Si) and C (SiO<sub>2</sub>) are demonstrated through the wavelengths of interest based on the experimental verifications of Schinke et al. and Rodríguez-de Marcos et al. (Schinke et al. 2015; Rodríguez-de Marcos et al. 2016).

### 3 Results and discussion

Here, we present the numerical results of our design based on the characteristic matrix method. Our numerical results illustrate the transmittance properties of our structure in the visible light region and electromagnetic waves are considered to incident normally on the face of the PC structure. The mainstay of this research study is focused on the role of HMM layers on structure transmittivity. In particular, the HMM is characterized by a hyperbolic dispersion due to the indefinite response of its permittivity. These characteristics could be of significant contribution to introducing the proposed multichannel optical filter. Meanwhile, the thicknesses of the constituent materials are chosen as,  $d_A = 40nm$ ,  $d_B = 80nm$  and  $d_C = 180nm$ .

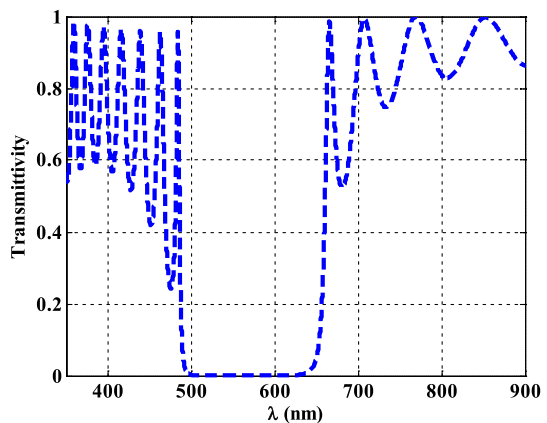
The numerical investigations highlight the role of the thicknesses of Ag, Si and SiO<sub>2</sub> besides the periodicity number of the HMM layer (N) and that of the whole configuration (S) on the structure transmittivity. In addition, we have discussed the effect of the refractive

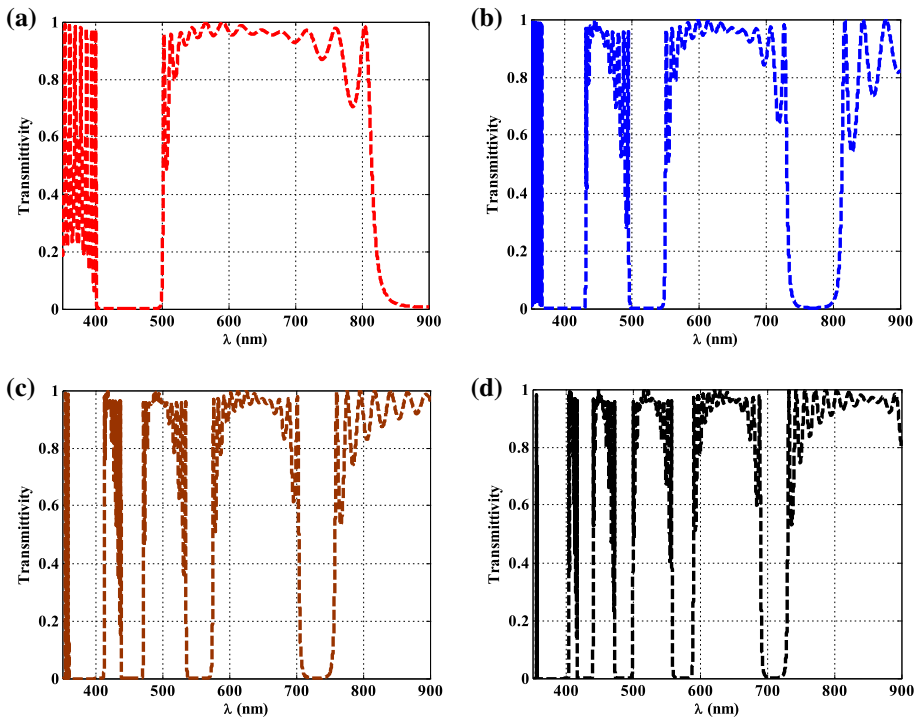
index of layer C on the transmittivity of our design. Firstly, we have discussed the variation of the periodicity number  $N$  and  $S$  on the structure transmittivity to obtain the optimum values of these parameters and their effect on the suggested multichannel optical filter.

Figure 2 clarifies the transmittivity of the designed structure at a periodicity number of the HMM=1 and that of the whole design=12. The figure shows the appearance of a single stop band that is located between 494.4 and 642.7 nm, respectively with a bandwidth=148.3 nm. Physically, the appearance of this PBG is due to the high mismatch in permittivity values of the constituent materials that leads to a multi-destructive interference at layers interfaces. Such strategy has the most significant contribution to the confinement of specified wavelengths of the incident electromagnetic waves leading to the formation of this PBG.

Next, we have discussed the role of the generation or periodicity number of the HMM on the tunability and characteristics of the formed PBG. In Fig. 3 we have plotted the transmission spectra of the 1DPCs against the wavelength of the incident electromagnetic wave at different numbers of periodicity for the HMM. Here, the periodicity number of the whole design is kept constant=12. The figure shows a crucial role of the HMM on the tunability of the PBG by changing the value of  $N$ . As  $N$  value increases from 1 to 2, the PBG has shifted downwards the shorter wavelengths and its width is reduced to 95 nm as shown in Fig. 3a. In addition, a wide passband region with a relatively high transmittivity appears in the wavelengths from 500 to 800 nm. For  $N=4$  and 6, the number of PBGs begins to increase significantly as shown in Fig. 3b, c, respectively. In the case of  $N=4$ , three PBGs are introduced as demonstrated in Fig. 3b. These stop bands are located at wavelengths from 363.9 to 430.6 nm, 498.5 nm to 546.8 nm and 742.5 nm to 801 nm, respectively. These band gaps may be attributed as a result of the contrast in the refractive index between the components of the PC structure. Therefore, such gaps could be the keystone of our optical stopbands optical filter. At  $N=6$ , the number of the investigated PBGs is still increasing to reach 4 as shown in Fig. 3c. Here, the widths of these gaps are decreased besides their shifting downwards the shorter wavelengths compared to the previous ones that appeared in Fig. 3a, b. For further increase in  $N$  value to 8, five PBGs are formed through the wavelengths of interest as shown in Fig. 3d. We believe that the increase in the periodicity number of HMM leads to the change in the optical path length of the incident waves. Thus, the transmittivity of the suggested design and PBGs as well are strongly affected by the variation in the values of  $N$ . Meanwhile, this parameter may

**Fig. 2** The transmittance of the designed structure as a function of the incident wavelength at  $N=1$  and  $S=12$





**Fig. 3** The transmittivity of the designed 1D HMM PCs at different values of the HMM periodicity such that, **a**  $N=2$ , **b**  $N=4$ , **c**  $N=6$  and **d**  $N=8$

be of great interest in the tunability of the PBGs characteristics such as their positions, widths, and numbers. Therefore, the periodicity number of HMM can provide a significant contribution toward the control of the number of channels for the suggested optical filter. In addition, the designed structure provides a kind of simplicity in the investigation of this role, unlike the previous works that could require some changes on the external parameters such as the doping impurity concentration or the permittivities of the considered materials (Elsayed 2018b).

Then, Fig. 4 elucidates the effect of the periodicity number of the whole design on the transmittivity properties. Here, the value of  $N$  is kept constant at the value of 6. The figure clarifies that the change in the periodicity of the whole structure has not led to a distinct effect on the structure transmittivity and the properties of the investigated PBGs as well. Here, the structure transmittivity and the characteristics of the formed PBGs are almost unaffected. We believe that this response is logical compared to the results that were investigated in the previous literature (Abadla et al. 2020; Elsayed et al. 2021; Mehaney et al. 2021). In particular, the role of the periodicity number is limited to producing more sharpness in the edges of the PBGs. Thus, we have considered the case of  $N=6$  and  $S=12$  as the optimum condition through this study.

Now, we study the effect of another parameter on the transmittivity of our designed structure. Figures 5 and 6 highlights the role of the thicknesses of Si, and Ag, respectively, on the characteristics of the stopbands of the optical filter. In particular, this parameter has a distinct contribution to control the optical path length of the incident electromagnetic



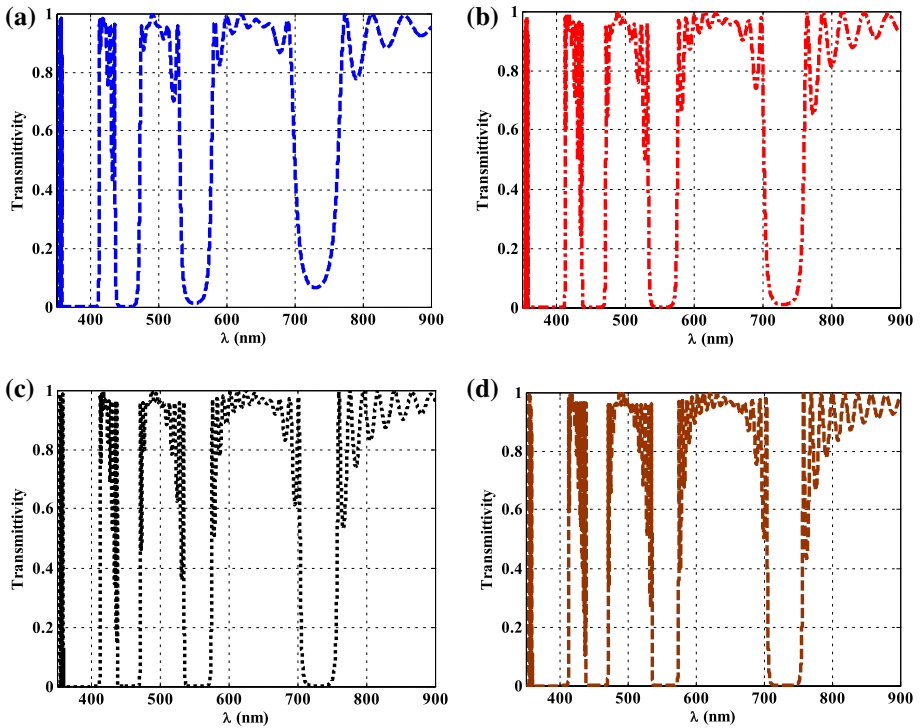


**Fig. 4** The transmittivity of the designed 1D HMM PCs at constant value of the HMM periodicity ( $N=6$ ) and different values of the periodicity number of the whole structure such that, **a**  $S=6$ , **b**  $S=9$ , **c**  $S=12$  and **d**  $S=15$

waves. Therefore, it could provide some flexibility in tuning the position of the introduced stopbands.

Figure 5 demonstrates the effect of Si thickness on the transmittance properties of our structure. Figure 5 shows the PBGs have red shifts toward longer wavelengths as a result of increasing the thickness of silicon from 40 to 60 nm, 80 nm, and 100 nm. In addition, the widths of these stopbands are slightly increasing with the increment in the thickness of Si layers. Also, the edges of these PBGs became sharper especially at the longer wavelengths.

Next, we discuss the effects of considering the different thicknesses of Ag layers at a constant value of  $d_A=40$  nm on the transmission properties of the PC as elucidated in Fig. 6. The figure indicates a significant effect of the thickness of Ag layers on the structure transmittivity and the properties of the PBGs as well. By decreasing the thickness of Ag from 80 to 60 nm and 40 nm, the structure transmittivity increases besides the shift in the positions of the formed PBGs downward the shorter wavelength (blue shifts) as shown in Fig. 6. Moreover, the widths of these gaps decrease, and their edges became less severe. Therefore, the choice of  $d_B=80$  nm represents the optimum value for sharper and wider stopbands.

Then, we investigated in Fig. 7 the role of the refractive index of layer C on the tunability of the obtained PBGs. Meanwhile, the values of  $d_A$  and  $d_B$  are equivalent to 40 nm and 80 nm, respectively. Such an effect could be established by comparing the  $\text{SiO}_2$  material (layer C) with other materials of different optical properties. As layer C

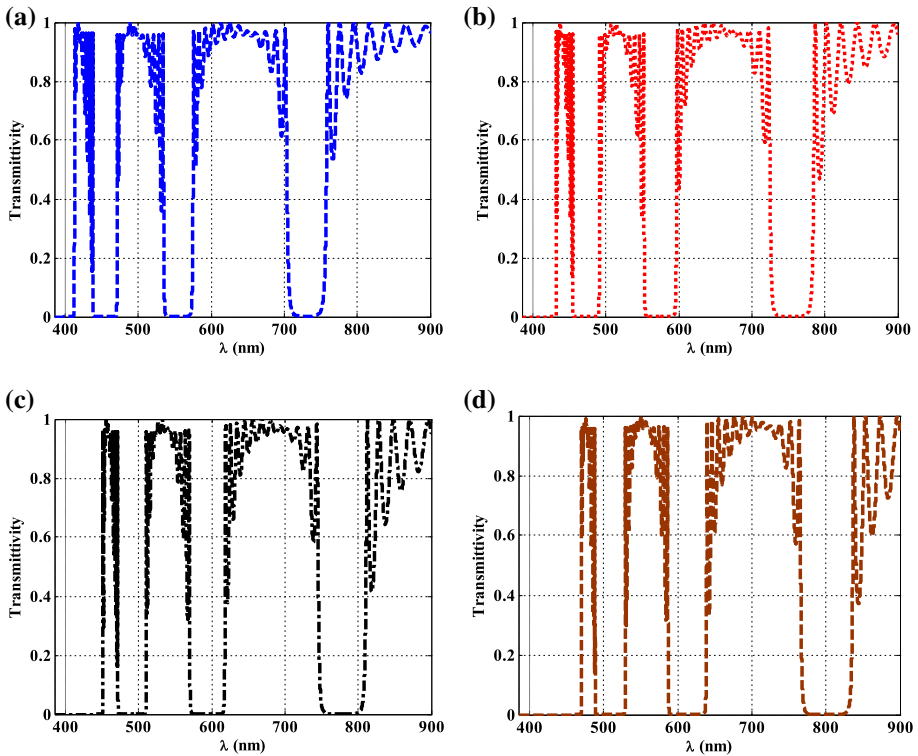


**Fig. 5** The structure transmittivity at different thicknesses of Si layers, **a**  $d_A=40$  nm, **b**  $d_A=60$  nm, **c**  $d_A=80$  nm and **d**  $d_A=100$  nm

is designed from  $\text{Al}_2\text{O}_3$ , the refractive index of this layer changes through the wavelengths of interest (Dodge 1986). This effect could lead to a distinct effect on the structure transmittivity as a result of changing the optical path length. Here, the change in the refractive index of layer C requires a similar change in the wavelength or the optical path length of the incident radiation to keep the state of constant phase shift that is ruled based on Bragg law (Segovia-Chaves and Elsayed 2021). Therefore, a different response of the structure transmittivity and the PBGs characteristics as well is expected. In this context, Fig. 7b demonstrates a different response as  $\text{SiO}_2$  was replaced with  $\text{Al}_2\text{O}_3$ . The figure clarifies distinct variations in the structure transmittivity and the properties of the obtained stopbands as well. Here, the obtained gaps are shifted upwards the longer wavelengths as a result of the changes in the optical wavelengths of the incident waves with the increase of the refractive index of layer C. In addition, the gaps in the longer wavelengths became less severe compared with the case of  $\text{SiO}_2$ . Moreover, the amplitudes of oscillations outside the PBGs take large values. As  $\text{Al}_2\text{O}_3$  is replaced with other optical materials such as  $\text{Si}_3\text{N}_4$  and ZnS, respectively, the shift towards the longer wavelengths is still present as shown in Fig. 7c, d, respectively. Furthermore, the number of the formed stopbands begins to decrease as obtained in the case of ZnS. In particular, the refractive indices of these materials ( $\text{Si}_3\text{N}_4$  and ZnS) along the wavelengths of interest have larger values compared with  $\text{Al}_2\text{O}_3$  (Luke et al. 2015; Klein et al. 1986).

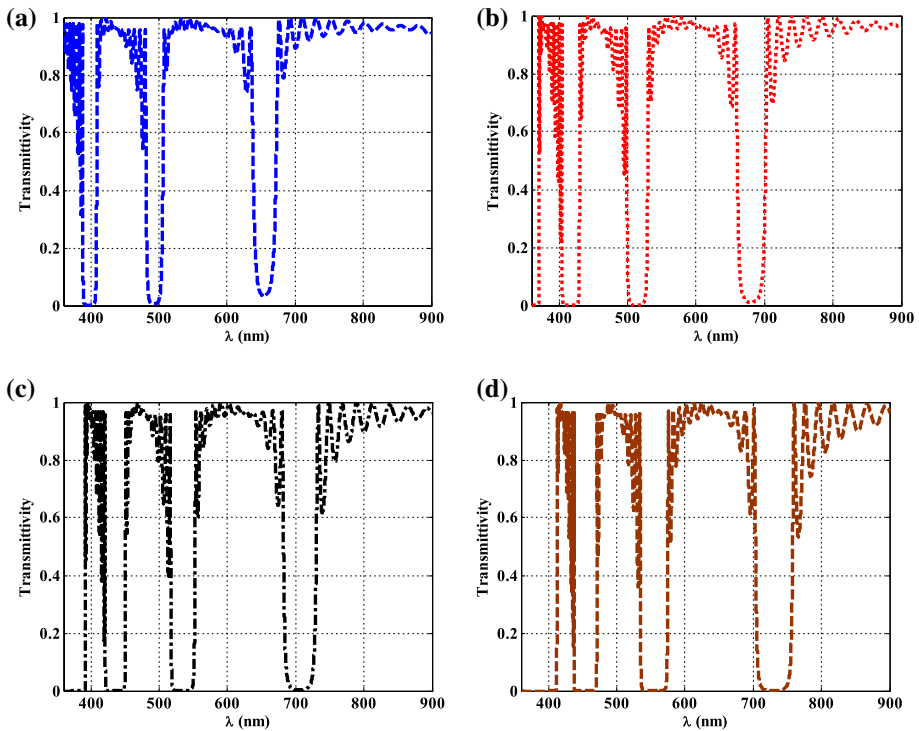


**Fig. 6** The effect of changing the thickness of Ag layers on the transmittance properties of the designed 1D HMM PCs at, **a**  $d_B = 20$  nm, **b**  $d_B = 40$  nm, **c**  $d_B = 60$  nm and **d**  $d_B = 80$  nm

Therefore, the utilization of  $\text{SiO}_2$  represents the optimum case to keep the largest number of stopbands through our proposed optical filter.

## 4 Conclusion

In summary, we have designed a multichannel optical filter based on a 1DPC comprising HMMs. The HMM was introduced as a combination of a periodic arrangement of Si and Ag layers. The numerical verifications of our study were introduced depending on the basics of Drude model, the effective medium theory, and the well-known characteristics matrix method. The demonstrated results showed the appearance of a multichannel stopband filter through the visible wavelengths especially at a periodicity number of the HMM layers greater than 1. In this regard, we have found that increasing the periodicity of HMM layers to 6 could lead to the formation of five PBGs with different bandwidths among the considered wavelengths. Moreover, the variation in the thickness of Ag and Si layers could have significant contributions towards the tunability of the positions and widths of these stopbands. Thus, these features of PBGs could make our proposed structure a prime candidate as a multichannel filter in a broad band of the visible light region.

**Acknowledgements** The authors extend their appreciation to the Deanship of Scientific Research at Jouf University for funding this work through research Grant No. (DSR-2021-03-0215).

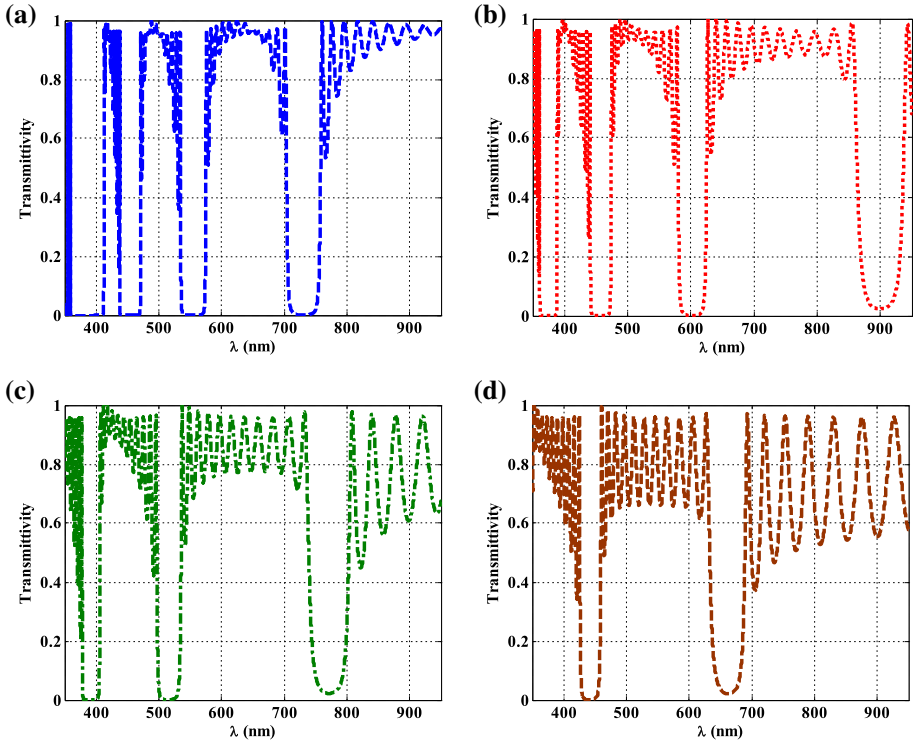


**Fig. 7** The effect of changing the refractive index of layer C on the structure transmittivity and the PBGs properties based on using different dielectric media such as, **a**  $\text{SiO}_2$ , **b**  $\text{Al}_2\text{O}_3$ , **c**  $\text{Si}_3\text{N}_4$  and **d**  $\text{ZnS}$

**Author contributions** MM and HAE conceived of the presented idea and developed the theory and performed the computations. AM wrote the manuscript with support from TAT, LShA, ZAA and HAE. All authors discussed the results and contributed to the final manuscript.

**Data availability** The data that support the findings of this study will be made available from the corresponding author upon reasonable request.

**Code availability** Not applicable.

## Declarations

**Conflict of interest** The authors declare they have no conflicts of interests.

**Consent to participate** All authors accepted.

**Consent for publication** All authors accepted.

**Ethical approval** I, hereby, the corresponding author declare that the authors have thoroughly read the Journal Policy and admitted all its requirements. Specifically, I declare here that this contribution is original and has not been published anywhere. I also declare that this article doesn't contain any plagiarized materials. No part of this manuscript has been introduced in any conference or published in any journal.

## References

- Abadla, M.M., Elsayed, H.A., Mehaney, A.: Thermo-optical properties of binary one dimensional annular photonic crystal including temperature dependent constituents. *Phys. E* **119**, 114020 (2020)
- Aghajamali, A., Barati, M.: Properties of defect modes in periodic lossy multilayer with negative-index-materials. *Commun. Theor. Phys.* **60**(1), 80–86 (2013)
- Aly, H., ElSayed, H.A.: Tunability of defective one-dimensional photonic crystals based on Faraday effect. *J. Mod. Opt.* **64**(8), 871–877 (2016)
- Aly, A.H., El-Naggar, S.A., Elsayed, H.A.: Tunability of two dimensional n-doped semiconductor photonic crystals based on the Faraday effect. *Opt. Express* **23**, 15038–15046 (2015)
- Aly, A.H., Aghajamali, A., ElSayed, H., Mobarak, M.: Analysis of cutoff frequency in a one-dimensional superconductor-metamaterial photonic crystal. *Phys. C Supercond. Appl.* **528**, 5–8 (2016)
- Awasthi, S.K., Mishra, A., Malaviya, U., Ojha, S.P.: Wave propagation in a one-dimensional photonic crystal with metamaterial. *Solid State Commun.* **149**(33–34), 1379–1383 (2009)
- Born, M., Wolf, E.: *Principles of Optics*. Cambridge, London (1999)
- Campione, S., Klem, J.F., Liu, S., Montano, I., Sinclair, M.B., Luk, T.S.: Experimental evidence of the lorentz-like effective medium resonance in semiconductor hyperbolic metamaterials using strong coupling to plasmonic metasurfaces. *IEEE Trans. Antennas Propag.* **68**, 1748–1754 (2020)
- Correas-Serrano, D., Gomez-Diaz, J.S., Tymchenko, M., Alù, A.: Nonlocal response of hyperbolic metasurfaces. *Opt. Express* **23**(23), 29434–29448 (2015)
- Cui, N., Guan, M., Mengke, Xu., Fang, W., Zhang, Y., Zhao, C., Zeng, Y.: Design and application of terahertz metamaterial sensor based on DSRRs in clinical quantitative detection of carcinoembryonic antigen. *Opt. Express* **28**, 16834–16844 (2020)
- Devashish, D., Ojambati, O.S., Hasan, S.B., van der Vegt, J.J.W., Vos, W.L.: Three-dimensional photonic band gap cavity with finite support: enhanced energy density and optical absorption. *Phys. Rev. B* **99**(7), 075112 (2019)
- Dodge, M.J.: Refractive index. In: *Handbook of Laser Science and Technology, Volume IV, Optical Materials: Part 2*, p. 30. CRC Press, Boca Raton (1986)
- Drexler, C., Shishkanova, T.V., Lange, C., Danilov, S.N., Weiss, D., Ganichev, S.D., Mirsky, V.M.: Terahertz split-ring metamaterials as transducers for chemical sensors based on conducting polymers: a feasibility study with sensing of acidic and basic gases using polyaniline chemosensitive layer. *Microchim. Acta* **181**, 1857–1862 (2014)
- Durach, M.: Tetra-hyperbolic and tri-hyperbolic optical phases in anisotropic metamaterials without magnetolectric coupling due to hybridization of plasmonic and magnetic Bloch high-k polaritons. *Opt. Commun.* **476**, 126349 (2020)
- Durach, M., Williamson, R., Laballe, M., Mulkey, T.: Tri- and tetrahyperbolic isofrequency topologies complete classification of bianisotropic materials. *Appl. Sci.* **10**, 763 (2020)
- Elsayed, H.A.: Transmittance properties of one dimensional ternary nanocomposite photonic crystals. *Mater. Res. Express* **5**, 036209 (2018a)
- Elsayed, H.A.: A multi-channel optical filter by means of one dimensional n doped semiconductor dielectric photonic crystals. *Mater. Chem. Phys.* **216**, 191–196 (2018b)
- Elsayed, H.A., Aly, A.H.: Terahertz frequency superconductor-nanocomposite photonic band gap. *Int. J. Mod. Phys. B* **32**, 1850056 (2017)
- Elsayed, H.A., Mehaney, A.: A new method for glucose detection using the one dimensional defective photonic crystals. *Mater. Res. Express* **6**, 036201 (2019)
- Elsayed, H.A., Mehaney, A.: Theoretical verification of photonic crystals sensor for biodiesel detection and sensing. *Phys. Scr.* **95**, 085507 (2020)
- Elsayed, H.A., Mehaney, A.: Monitoring of soybean biodiesel based on the one-dimensional photonic crystals comprising porous silicon. *Appl. Nanosci.* **11**, 149–157 (2021)
- Elsayed, H.A., El-Naggar, S.A., Aly, A.H.: Thermal properties and two-dimensional photonic band gaps. *J. Mod. Opt.* **61**, 385–389 (2014)
- Elsayed, H.A., Sayed, F.A., Aly, A.: Graphene deposited liquid crystal and thermal sensitivity using photonic crystals. *Phys. Scr.* **96**, 035503 (2021)
- Fesenko, V.I., Tuz, V.R.: Lossless and loss-induced topological transitions of isofrequency surfaces in a biaxial gyroelectromagnetic medium. *Phys. Rev. B* **99**, 094404 (2019)
- Fietz, C., Urzhumov, Y., Shvets, G.: Complex k band diagrams of 3D metamaterial/photonic crystals. *Opt. Express* **19**, 19027–19041 (2011)
- Gaspar-Armenta, J.A., Villa, F.: Photonic surface-wave excitation: photonic crystal–metal interface. *JOSA B* **20**(11), 2349–2354 (2003)

- Guo, Z., Jiang, H., Chen, H.: Hyperbolic metamaterials: From dispersion manipulation to applications. *J. Appl. Phys.* **127**, 071101 (2020)
- Haakestad, M., Alkeskjold, T., Nielsen, M., Scolari, L., Riishede, J., Engan, H., Bjarklev, A.: Electrically tunable photonic bandgap guidance in a liquid-crystal-filled photonic crystal fiber. *IEEE Photon. Technol. Lett.* **17**, 819–821 (2005)
- Hadfield, R.H.: Single-photon detectors for optical quantum information applications. *Nat. Photon* **3**(12), 696–705 (2009)
- Haring Bolivar, P., Nagel, M., Richter, F., Brucherseifer, M., Kurz, H., Bosserhoff, A., Buttner, R.: Label-free THz sensing of genetic sequences: towards “THz biochips.” *Philos. Trans. r. Soc. Math. Phys. Eng. Sci.* **362**(1815), 323–335 (2004)
- Hu, S., Song, J., Guo, Z., Jiang, H., Deng, F., Dong, L., Chen, H.: Omnidirectional nonreciprocal absorber realized by the magneto-optical hypercrystals. *Opt. Express* **30**(7), 12104–12119 (2022)
- Huo, P., Zhang, Si., Liang, Y., Lu, Y., Xu, T.: Hyperbolic metamaterials and metasurfaces: fundamentals and applications. *Adv. Opt. Mater.* **7**, 1801616 (2019)
- Istrate, E., Sargent, E.H.: Photonic crystal heterostructures and interfaces. *Rev. Mod. Phys.* **78**, 455–481 (2006)
- Janaszek, B., Kieliszczyk, M., Tyszka-Zawadzka, A., Szczepański, P.: Multiresonance response in hyperbolic metamaterials. *Appl. Opt.* **57**(9), 2135–2141 (2018)
- Joannopoulos, J.D., Johnson, S.G., Winn, J.N., Meade, R.D.: *Photonic Crystals: Molding the Flow of Light*. Princeton Univ. Press, Princeton (2008)
- John, S.: Strong localization of photons in certain disordered dielectric superlattices. *Phys. Rev. Lett.* **58**(23), 2486–2489 (1987)
- Johnson, P.B., Christy, R.W.: Optical constants of the noble metals. *Phys. Rev. B* **6**, 4370–4379 (1972)
- Klein, C.A.: Room-temperature dispersion equations for cubic zinc sulfide. *Appl. Opt.* **25**, 1873–1875 (1986)
- Li, J., Zhou, L., Chan, C.T., Sheng, P.: Photonic band gap from a stack of positive and negative index materials. *Phys. Rev. Lett.* **90**(8), 083901 (2003)
- Li, D., Lin, S., Hu, F., Chen, Z., Zhang, W., Han, J.: Metamaterial terahertz sensor for measuring thermal-induced denaturation temperature of insulin. *IEEE Sens. J.* **20**(4), 1821–1828 (2020)
- Lin, W.-H., Wu, C.-J., Yang, T.-J., Chang, S.-J.: Terahertz multichanneled filter in a superconducting photonic crystal. *Opt. Express* **18**(26), 27155–27166 (2010)
- Luke, K., Okawachi, Y., Lamont, M.R.E., Gaeta, A.L., Lipson, M.: Broadband mid-infrared frequency comb generation in a Si<sub>3</sub>N<sub>4</sub> microresonator. *Opt. Lett.* **40**, 4823–4826 (2015)
- Mehaney, A., Alrowaili, Z.A., Elsayed, H.A., Taha, T.A., Ahmed, A.M.: Theoretical investigations of Tamm plasmon resonance for monitoring of isoprene traces in the exhaled breath: towards chronic liver fibrosis disease biomarkers. *Phys. Lett. A* **413**, 127610 (2021)
- Noda, S., Baba, T. (eds.): *Roadmap on Photonic Crystals*, vol. 1. Springer, New York (2003)
- Noda, S., Imada, M., Okano, M., Ogawa, S., Mochizuki, M., Chutinan A.: Semiconductor three-dimensional and two-dimensional photonic crystals and devices. *IEEE J. Quantum Electron.* **38**, 726–735 (2002)
- Notomi, M., Shinya, A., Mitsugi, S., Kira, G., Kuramochi, E., Tanabe, T.: Optical bistable switching action of Si high-Q photonic-crystal nanocavities. *Opt. Express* **13**(7), 2678–2687 (2005)
- Poddubny, A., Iorsh, I., Belov, P., Kivshar, Y.: Hyperbolic metamaterials. *Nat. Photonics* **7**, 948–957 (2013)
- Podolskiy, V.A., Elser, J., Salakhutdinov, I., Avrutsky, I.: Nonlocal effects in effective medium response of nanolayered metamaterials. *Appl. Phys. Lett.* **90**, 191109 (2007)
- Porrás-Montenegro, N., Duque, C.A.: Temperature and hydrostatic pressure effects on the photonic band structure of a 2D honeycomb lattice. *Phys. E* **42**(6), 1865–1869 (2010)
- Ramanujam, N.R., Joseph Wilson, K.S., Mahalakshmi, P., Taya, S.A.: Analysis of photonic band gap in photonic crystal with epsilon negative and double negative materials. *Optik* **183**, 203–210 (2019)
- Rodríguez-de Marcos, L.V., Larroquet, J.I., Méndez, J.A., Aznárez, J.A.: Self-consistent optical constants of SiO<sub>2</sub> and Ta<sub>2</sub>O<sub>5</sub> films. *Opt. Mater. Express* **6**, 3622–3637 (2016)
- Sánchez, A.S., Halevi, P.: Simulation of tuning of one-dimensional photonic crystals in the presence of free electrons and holes. *J. Appl. Phys.* **94**(1), 797–799 (2003)
- Schinke, C., Peest, P.C., Schmidt, J., Brendel, R., Bothe, K., Vogt, M.R., Kröger, I., Winter, S., Schirmacher, A., Lim, S., Nguyen, H.T., MacDonald, D.: Uncertainty analysis for the coefficient of band-to-band absorption of crystalline silicon. *AIP Adv.* **5**, 67168 (2015)
- Segovia-Chaves, F., Elsayed, H.A.: Pressure-based defect mode tunability in a one-dimensional photonic crystal composed of SiO<sub>2</sub> and Si. *Optik* **247**, 167802 (2021)

- Shalin, A.S., Ginzburg, P., Orlov, A.A., Iorsh, I., Belov, P.A., Kivshar, Y.S., Zayats, A.V.: Scattering suppression from arbitrary objects in spatially dispersive layered metamaterials. *Phys. Rev. B* **91**(12), 125426 (2015)
- Smith, D., Padilla, W., Vier, D., Nemat-Nasser, S., Schultz, S.: Composite medium with simultaneously negative permeability and permittivity. *Phys. Rev. Lett.* **84**(18), 4184–4187 (2000)
- Takeda, H., Yoshino, K.: Tunable photonic band gaps in two-dimensional photonic crystals by temporal modulation based on the Pockels effect. *Phys. Rev. E* **69**(1), 016605 (2004)
- Trabelsi, Y., Ben Ali, N., Segovia-Chaves, F., Posada, H.V.: Photonic band gap properties of one-dimensional photonic quasicrystals containing nematic liquid crystals. *Results in Phys.* **19**, 103600 (2020)
- Tuz, V.R., Fesenko, V.I.: Magnetically induced topological transitions of hyperbolic dispersion in biaxial gyrotropic media. *J. Appl. Phys.* **128**, 013107 (2020)
- Veselago, V.G.: The electrodynamics of substances with simultaneously negative values of  $\epsilon$  and  $\mu$ . *Sov. Phys. Usp.* **10**, 509–514 (1968)
- Wu, C., Chien-Jang, Y., Chung, Y.-H., Syu, B.-J., Yang, T.-J.: Band gap extension in a one-dimensional ternary metal-dielectric photonic crystal. *Prog. Electromag. Res.* **102**, 81–93 (2010a)
- Wu, C.J., Liao, J.J., Chang, T.W.: Tunable multilayer Fabry-Perot resonator using electro-optical defect layer. *J. Electromag. Waves Appl.* **24**, 531–542 (2010b)
- Wu, F., Lu, G., Xue, C., Jiang, H., Guo, Z., Zheng, M., Chen, C., Du, G., Chen, H.: Experimental demonstration of angle-independent gaps in one-dimensional photonic crystals containing layered hyperbolic metamaterials and dielectrics at visible wavelengths. *Appl. Phys. Lett.* **112**, 041902 (2018)
- Wu, F., Zhang, X., Liu, D., Yin, C.: Angle-insensitive phase shift in one-dimensional photonic crystal containing hyperbolic metamaterials in the visible range. *Phys. B* **639**, 413967 (2022)
- Xu, C., Hu, X., Li, Y., Liu, X., Fu, R., Zi, J.: Semiconductor-based tunable photonic crystals by means of an external magnetic field. *Phys. Rev. B* **68**(19), 193201 (2003)
- Xue, C., Ding, Y., Jiang, H., Li, Y., Wang, Z., Zhang, Y., Chen, H.: Dispersionless gaps and cavity modes in photonic crystals containing hyperbolic metamaterials. *Phys. Rev. B* **93**, 125310 (2016)
- Yablonovitch, E.: Inhibited spontaneous emission in solid-state physics and electronics. *Phys. Rev. Lett.* **58**(20), 2059–2062 (1987)
- Zhao, D., Meng, L., Gong, H., Chen, X., Chen, Y., Yan, M., Li, Q., Qiu, M.: Ultra-narrow-band light dissipation by a stack of lamellar silver and alumina. *Appl. Phys. Lett.* **104**, 221107 (2014)
- Zheng, Z., Liu, X., Luo, Y., Cheng, B., Zhang, D., Meng, Q., Wang, Y.: Pressure controlled self-assembly of high quality three-dimensional colloidal photonic crystals. *Appl. Phys. Lett.* **90**(5), 051910 (2007)

**Publisher's Note** Springer Nature remains neutral with regard to jurisdictional claims in published maps and institutional affiliations.

Springer Nature or its licensor (e.g. a society or other partner) holds exclusive rights to this article under a publishing agreement with the author(s) or other rightsholder(s); author self-archiving of the accepted manuscript version of this article is solely governed by the terms of such publishing agreement and applicable law.